# Seasonal variations in planktonic foraminiferal flux and oxygen isotopic composition in the western North Pacific: implications for paleoceanographic reconstruction

**Takuya Sagawa***

*Senior Research Fellow Center, Ehime University, 2-5 Bunkyo-cho, Matsuyama, Ehime, 790-0826, Japan*

(*Corresponding author. Tel&Fax: +81-89-927-9654, e-mail: tsagawa@sci.ehime-u.ac.jp)

**Azumi Kuroyanagi**

*Atmosphere and Ocean Research Institute, The University of Tokyo, 5-1-5 Kashiwanoha, Kashiwa, Chiba, 277-8564, Japan* (e-mail: a-kuroyanagi@aori.u-tokyo.ac.jp)

**Tomohisa Irino**

*Faculty of Environmental Earth Science, Hokkaido University, N10W5 Kita-ku, Sapporo, Hokkaido, 060-0810, Japan* (e-mail: irino@ees.hokudai.ac.jp)

**Michinobu Kuwae**

*Senior Research Fellow Center, Ehime University, 2-5 Bunkyo-cho, Matsuyama, Ehime, 790-0826, Japan* (e-mail: mkuwae@sci.ehime-u.ac.jp)

**Hodaka Kawahata**

*Atmosphere and Ocean Research Institute, The University of Tokyo, 5-1-5 Kashiwanoha, Kashiwa, Chiba, 277-8564, Japan* (e-mail: kawahata@aori.u-tokyo.ac.jp)

## Abstract

The oxygen isotopic composition ($\delta^{18}O$) of planktonic foraminiferal shells in seafloor sediment provides information on past surface oceanography. Knowledge of seasonal and depth habitat, as well as the $\delta^{18}O$ disequilibrium (vital effect), is essential to constrain the interpretation of sedimentary $\delta^{18}O$. Here, we present a 1-year time series of planktonic foraminiferal shell fluxes and $\delta^{18}O$ from a sediment trap moored in the northwestern margin of the North Pacific. The vital effect and calcification depth for four species were estimated by comparing shell $\delta^{18}O$ and the predicted values of equilibrium calcite calculated from temperature and estimated $\delta^{18}O$ in seawater. Six major species (*Neogloboquadrina incompta*, *Neogloboquadrina dutertrei*, *Neogloboquadrina pachyderma*, *Globigerina quinqueloba*, *Globigerina bulloides*, and *Globorotalia scitula*) constituted 97% of the total foraminiferal flux. Most major species showed large fluxes in June and December, corresponding to periods of the development and disruption of the seasonal thermocline, implying the importance of nutrient injection and/or circulation for foraminiferal fluxes. Additional peaks in *N. dutertrei* and *N. pachyderma* were observed in August. The seasonal successions of foraminiferal fluxes corresponded to surface ocean stratification conditions and food availability, which are closely related to circulation of local currents. Vital effect estimations suggest that shells calcified in equilibrium for *G. bulloides* and *N. pachyderma* [sinistral (s)] and with a –0.7‰ offset for *N. dutertrei* [dextral (d)], a –1.0‰ offset for *N. incompta* (d), and a –0.3‰ offset for *N. pachyderma* (d).

45 The calculation of flux-weighted $\delta^{18}O$ values reveals that the sedimentary $\delta^{18}O$ values of *G.*
46 *bulloides*, *N. dutertrei* (d), and *N. incompta* (d) reflect surface temperature in winter season, and
47 those of *N. pachyderma* (s) and *N. pachyderma* (d) reflect summer and annual mean subsurface
48 temperature, respectively. The shallow calcification depths for the four species suggest that $\delta^{18}O$
49 between different species ($\Delta\delta^{18}O$) in the western North Pacific does not work for reconstructing past
50 stratification conditions, unlike in other regions. Rather, the $\Delta\delta^{18}O$ between *N. pachyderma* (s) and *G.*
51 *bulloides*, *N. dutertrei* (d) or *N. incompta* (d) would provide a proxy for past seasonality.
52
53 *Keywords: planktonic foraminifera, sediment traps, oxygen isotopes, northwestern North Pacific*
54

## 1. Introduction

The oxygen isotopic composition ($\delta^{18}O$) of planktonic foraminifera has been widely used to reconstruct past surface ocean conditions. Because the isotopic fractionation factor between water and carbonate minerals depends on the calcification temperature (e.g., Epstein et al., 1953; McCrea, 1950), $\delta^{18}O$ in fossil foraminifera in seafloor sediments records both past seawater $\delta^{18}O$ and temperature changes. Knowledge of the seasonal and depth habitats of foraminifera is essential when fossil $\delta^{18}O$ is used for paleoceanographic reconstruction. Additionally, the difference in $\delta^{18}O$ among species ($\Delta\delta^{18}O$) that live different depths or seasonal habitats may give us an opportunity to investigate past stratification (e.g., Mortyn et al., 2002; Mulitza et al., 1997; Rashid and Boyle, 2007; Sagawa et al., 2011; Simstich et al., 2003; Spero et al., 2003) or seasonality (Jonkers et al., 2010). The vertical and seasonal distributions of planktonic foraminifera are strongly affected by regional environmental factors, such as geography, hydrography, and ecosystems (e.g., Fairbanks et al., 1980; Kuroyanagi and Kawahata, 2004; Kuroyanagi et al., 2002; Sautter and Thunell, 1991). The regional environment may also influence the vital effect of the shell $\delta^{18}O$ (e.g., Niebler et al., 1999), which is defined as offset from the $\delta^{18}O$ equilibrium value. It is therefore important to constrain the influences of habitat distribution and the vital effect in the fossil $\delta^{18}O$ records on regional scales.

The planktonic foraminiferal species *Neogloboquadrina pachyderma* (Ehrenberg) has been

commonly used in paleoceanographic studies of the middle to high latitudes. Temporal variation in the coiling ratio of this species has been interpreted in relation to past environmental changes (e.g., Thompson and Shackleton, 1980). However, recent genetic studies revealed that the two morphospecies with opposite coiling directions show distinct genetic patterns (Bauch et al., 2003; Darling et al., 2000). Based on the genetic differences and geographic distribution of the morphospecies, Darling et al. (2006) suggested that the right-coiling morphospecies should be recognized as *Neogloboquadrina incompta* (Cifelli). The geographic distribution of *N. pachyderma* and *N. incompta* in surface sediments around the Japanese islands also shows a distinct pattern (Oda and Domitsu, 2009; and references therein). In general, the left-coiling form is dominant in *N. pachyderma* and the right-coiling form is dominant in *N. incompta* (Darling et al., 2006; Oda and Domitsu, 2009), accounting for >97% in both species. However, a higher right-coiling ratio (>50%) in *N. pachyderma*, which is distinct from *N. incompta*, was reported from the Holocene sediment of the northwestern margin of the North Pacific (Kuroyanagi et al., 2006). This evidence implies that the coiling direction–based identification method is not applicable to this region. Therefore, added understanding of the habitat preferences and $\delta^{18}O$ of these morphospecies is essential for paleoceanographic interpretation.

This study investigated the seasonal variation in the planktonic foraminiferal flux and $\delta^{18}O$ using a 1-year data series from a moored sediment trap in the northwestern margin of the North

Pacific (Fig. 1). The vital effect of $\delta^{18}O$, calcification depth, and flux-weighted $\delta^{18}O$ were estimated to better constrain the foraminiferal $\delta^{18}O$ proxy in paleoceanographic study. Our results revealed that differences in the flux-weighted $\delta^{18}O$ values among species mainly reflect seasonal flux pattern rather than the calcification depth in the western North Pacific, and the potential of $\Delta\delta^{18}O$ as a proxy of past seasonality in this region is therefore extended.

## 2. Oceanographic setting

The surface water around the study site is characterized by high seasonal variability due to the coexistence of the Oyashio Current and the Tsugaru Warm Current (TGC; Fig. 1). The Oyashio Current is a western boundary current of the Western Subarctic Gyre of the North Pacific that transports cold, fresh surface water. The Oyashio Current off the southeastern coast of Hokkaido bifurcates into the first branch of the Oyashio and the coastal Oyashio Water (Kono et al., 2004). The TGC is relatively warm and saline (>6 °C and ~34.0) (Hanawa and Mitsudera, 1986) and it originates from the Tsushima Warm Current (TWC), which is formed by mixing of the Kuroshio water and the coastal water in the East China Sea. Changes in the relative influence of these currents produce strong seasonality in surface conditions. The first branch of the Oyashio Current reaches its southernmost latitude in late winter to early spring and its northernmost latitude in late summer to autumn (Yasuda, 2003). The influence of the TGC on the study site increases in summer and autumn

(Hanawa and Mitsudera, 1986).

Monthly mean vertical profiles of temperature, salinity, and density during the period corresponding to trap deployment, from May 2002 to May 2003, are shown in Fig. 2a–c. Temperature and salinity data were obtained from the National Centers for Environmental Prediction (NCEP) Global Ocean Data Assimilation System (GODAS) (Behringer and Xue, 2004). The temperature and salinity of the upper 200 m in March were nearly constant and fell within the range of about 2°C and 0.02, respectively, due to vertical mixing. Summer surface temperature reaches ~20°C and a steep thermocline develops at 20–40 m. The similarity of the density and temperature profiles suggests primary control by temperature, as expected with low variation in annual salinity (Fig. 2b).

## 3. Materials and Methods

### *3.1. Samples*

A time-series sediment trap (model SMD21-6000; Nichiyu-giken-kogyou Ltd., Tokyo, Japan) was deployed at 350 m water depth (~620 m above the seafloor) at 41°33.8’N, 141°52.0’E. The sediment trap has a collection area of 0.5 $m^2$ with 21 cup collectors and was moored for 1 year from June 2002 to June 2003. Each sample represents a collection period of 11–30 days, with most being 14 days (Kawahata et al., 2009). The sample treatments were conducted following a method

described in Kawahata et al. (1998). Prior to trap deployment, the sampling bottles were filled with filtered seawater (0.45 μm pore size) containing a 3% formalin solution buffered with sodium borate to retard microbial activity in the trapped sample. After recovery, samples were stored at 2–4°C. They were filtered through a 1-mm mesh to remove zooplanktonic swimmers. The <1-mm fraction was split into 64 aliquots. Major components of trap samples were reported by Kawahata et al. (2009).

### *3.2. Analytical Methods*

Planktonic foraminifera were wet sieved into two size fractions (125–250 μm and >250 μm), picked after drying, and identified for faunal abundance analysis. In this study, the taxonomic criteria followed Parker (1962), Saito et al. (1981), and Hemleben et al. (1989). $\delta^{18}O$ measurements were derived from four planktonic foraminiferal species: *Globigerina bulloides*, *Neogloboquadrina dutertrei* [dextral (d)], *N. incompta* (d), and *N. pachyderma* [dextral and sinistral (s)]. Identified foraminiferal shells (125–250 μm) were cleaned with a wet brush under a microscope before being measured. Ten specimens were ideally used for each measurement, but approximately half of the samples contained <10 shells (2–9 specimens). Measurements were obtained using an isotope mass spectrometer (Finnigan MAT 253; Thermo Fisher Scientific Inc.) connected to an automated preparation system (Kiel Carbonate device IV) at Hokkaido University. Measured results were

145 calibrated with the NBS-19 standard, which was analyzed in the same sequence, and expressed in

146 the VPDB scale. The analytical error was ± 0.06‰.

147

148 ### *3.3. Calculation of isotopic equilibrium and flux-weighted $\delta^{18}O$ values*

149 The predicted $\delta^{18}O$ value of equilibrium calcite was calculated using the $\delta^{18}O$ temperature

150 scale of Kim and O'Neil (1997):

151 $$\delta c = \frac{4.64 - \sqrt{21.53 - 0.36 \times (16.1 - T)}}{0.18} + \delta w \quad (1)$$

152 where $T$ is temperature (°C) and δc and δw are $\delta^{18}O$ values of carbonate and the ambient water,

153 respectively, relative to the VPDB. We chose this $\delta^{18}O$ temperature scale because the calibrated

154 temperature range (10-40ºC) corresponds to that of natural variability. When we discuss the vital

155 effect offset, it is reasonable to compare the measured values against the equilibrium $\delta^{18}O$ values

156 based on the inorganic precipitation relationship (Kim and O'Neil, 1997) rather than the values based

157 on field and laboratory relationships for specific foraminiferal taxa (e.g., Bemis et al., 1998; von

158 Langen et al., 2000) or mollusks (e.g., Epstein et al., 1953). Monthly mean temperature and salinity

159 data at 10-m depth intervals from 5 m to 303 m were obtained from a 1° × 1° gridded dataset of the

160 NCEP GODAS (Fig. 2a, b). Unfortunately, the GODAS has no temperature and salinity data for a

161 grid including the mooring site centered at 41°10’N, 141°30’E; therefore, average values were

162 calculated from three adjacent grids (Fig. 1b). Seawater $\delta^{18}O$ was estimated using the linear

relationship proposed by Oba and Murayama (2004) between salinity and δw in the Kuroshio-Oyashio mixed water region along the eastern coast of the Japanese islands:

$$\delta w = 0.521 \times S - 17.955, \quad (2)$$

where δw is $\delta^{18}O$ of seawater (VSMOW) and S is salinity. The δw is converted to the VPDB scale by subtracting 0.27‰ (Hut, 1987). The vertical distribution of the predicted $\delta^{18}O$ record inversely resembles that of temperature (Fig. 2), suggesting that the predicted $\delta^{18}O$ is controlled mainly by temperature.

To constrain the effect of the seasonal foraminiferal flux in the fossil $\delta^{18}O$ record, flux-weighted $\delta^{18}O$ values (King and Howard, 2005; Kuroyanagi et al., 2011) were calculated for each species using the following equation:

$$\text{Flux-weighted } \delta^{18}O \text{ value} = \sum_{i=1}^{n} (flux_i \times \delta^{18}O_i) / total\ flux \quad (3)$$

where $flux_i$ and $\delta^{18}O_i$ are the shell flux and $\delta^{18}O$ value for each species (125–250 μm size fraction).

## 4. Results

### *4.1. Seasonal fluxes*

Fluxes in major components of trapped particles are reported by Kawahata et al. (2009) (Fig. 3a–e). In general, major components showed higher fluxes during three periods: June–July 2002, October 2002–January 2003 (maximum in December), and April–May 2003. Total foraminiferal

shell flux (TFF) ranged from 2 to 2032 shells $m^{-2}$ $day^{-1}$ during the mooring period (Fig. 3f). Most (89%) of the TFF was composed of small individuals (125–250 μm). Seasonal variation in TFF differed slightly from that of other biogenic components. Higher TFFs were observed in June, August, and December 2002 and a small peak was observed in late May. Two peaks in June and December corresponded to higher fluxes for other biogenic components. However, a TFF peak observed in August was not accompanied by other components, which showed minimum fluxes at this time. Another difference is that the increase in TFF starting in late May 2003 lagged behind that of biogenic opal and organic matter. The beginning of the TFF increase also lagged behind that of carbonate flux, suggesting differences in biological response between foraminifera and coccolithophores.

A total of 14 planktonic foraminiferal species were found at this site. The fauna consisted mainly of the temperate and subpolar species *N. incompta*, *N. dutertrei*, *N. pachyderma*, *Globigerina quinqueloba*, *G. bulloides*, and *Globorotalia scitula*, which had relative abundances of 25.7%, 25.4%, 22.8%, 15.1%, 4.1%, and 3.7%, respectively. These six species made up more than 97% of annual TFFs (>125 μm). The seasonal fluxes for *G. bulloides*, *N. incompta*, and *G. quinqueloba* exhibited bimodal peaks: late spring–summer (May–June) and early winter (December; Fig. 4). An additional peak in August was significant for *N. dutertrei* and *N. pachyderma*. *Globorotalia scitula* had a prominent peak around August–September only. To evaluate differences in seasonal variation

199 between right- and left-coiling individuals, we examined the coiling ratios of *N. incompta*, *N.*
200 *dutertrei*, and *N. pachyderma*. *N. incompta* and *N. dutertrei* had high right-coiling ratios throughout
201 the sampling period (both annual mean values were 87%). In contrast, left-coiling individuals were
202 dominant in *N. pachyderma* (mean right-coiling ratio was 42%). Both coiling directions in all three
203 species had similar seasonal flux patterns; weak positive correlations were found between right- and
204 left-coiling fluxes ($r$ = 0.37, 0.44, and 0.58 in *N. incompta*, *N. dutertrei*, and *N. pachyderma*,
205 respectively).
206
207 ### *4.2. Measured shell $\delta^{18}O$ and predicted $\delta^{18}O$ equilibrium value*
208 Because the foraminiferal flux varied significantly with seasons, about half of the samples
209 consist of less than 10 specimens per measurement. In order to assess the representativeness of the
210 $\delta^{18}O$ measurement with a small number of foraminiferal tests, we conducted replicate analyses using
211 samples that contained enough foraminiferal tests. Figure 5 shows the results of the replicate
212 analyses of *N. pachyderma* (s) and *N. pachyderma* (d). Each measurement consists of 4-13
213 specimens with mostly less than 10 specimens. The results show that the reproducibility is generally
214 less than ±0.3‰ (1σ). This is much smaller than the seasonal $\delta^{18}O$ variations (Fig. 6), confirming the
215 reliability of $\delta^{18}O$ measurements with a small number of tests.
216 Measured shell $\delta^{18}O$ values for four species showed seasonal variation, with lighter values

obtained during summer and heavier values during winter and spring (Fig. 6). The $\delta^{18}O$ for all species was minimal in October, whereas the timing of the maximum value differed among species. More enriched values were observed in May for *G. bulloides* and *N. pachyderma* (s), in March for *N. incompta* (d), in late December for *N. pachyderma* (d), and in late June and February–March for *N. dutertrei*.

Predicted $\delta^{18}O$ values for equilibrium calcite calculated using GODAS temperature and salinity data showed clear seasonal succession, especially at shallower depths (Fig. 6). The seasonal amplitudes were 3.5‰ at 5 m, 0.6‰ at 105 m, and <0.3‰ at >155 m, reflecting larger temperature variation at shallower depth. The predicted $\delta^{18}O$ values at the end of winter were maximal and homogeneous for the upper 75 m due to deepening of the mixed layer. Minimum values at shallower depths (<15 m) were seen in August and September, whereas those at deeper depths (>25 m) lagged behind until October or November. This finding is explained by seasonal changes in the vertical thermal structure (Fig. 3g). The warming of surface water during summer produces strong stratification, which prevents subsurface warming in this season. Stratification decays gradually starting in October until isothermal conditions are achieved by late winter / early spring.

Measured shell $\delta^{18}O$ values for four species showed seasonal variation, with lighter values obtained during summer and heavier values during winter and spring (Fig. 5). The $\delta^{18}O$ for all species was minimal in October, whereas the timing of the maximum value differed among species. More

enriched values were observed in May for *G. bulloides* and *N. pachyderma* (s), in March for *N. incompta* (d), in late December for *N. pachyderma* (d), and in late June and February–March for *N. dutertrei*.

## 5. Discussion

### *5.1. Seasonal flux variations*

As mentioned above, the general seasonal patterns of the major foraminiferal species included two large maxima in summer (May–August) and early winter (December) and a small, broad maximum around autumn. In particular, *N. incompta* (both coiling directions), *G. quinqueloba*, and *G. bulloides* had almost the same seasonal peaks (May–June and December). These peak periods are consistent with the development and disruption of thermoclines (Fig. 3g), corresponding to periods before and after the TGC-dominant interval. Therefore, these results suggest that similar factors control seasonal fluxes in these three species (i.e., nutrients, light, food availability and/or water column structure). Similar seasonal flux patterns of *G. quinqueloba* and *G. bulloides* were also observed in the western North Pacific (Kuroyanagi et al., 2008). Concurrent increases with biogenic components (Fig. 3) and neritic radiolarian fluxes (Itaki et al., 2008) suggest that these species respond to nutrient-rich water. The supply of nutrients by vertical mixing and/or from coastal water might increase primary production and subsequent planktonic foraminiferal production.

*Neogloboquadrina dutertrei* (both coiling directions) showed a relatively large flux peak in

253 August. Hilbrecht (1997) reported two populations of *N. dutertrei*, tropical and subtropical. Plankton
254 tow experiments also showed bimodal peaks in the abundance of *N. dutertrei* (at ~18°C and 8°C)
255 around Japan (Kuroyanagi and Kawahata, 2004). Therefore, it is suggested that different populations
256 contribute to bimodal distribution in seasonal flux at this site. The maximum flux in summer was
257 reported from a sediment trap study at offshore site Sta. B (Fig. 1) (Itou and Noriki, 2002). In
258 contrast, the Japan Sea sediment trap showed a distinct peak of this species in November–December
259 (Park and Shin, 1998). These results suggest that the mid-summer and early winter peaks represent
260 the Pacific and Japan Sea populations, respectively.

261 Right-coiling *N. pachyderma* showed a large peak in August that decreased until January with
262 moderate fluctuations. In contrast, the left-coiling variety exhibited a large peak around June–August
263 and a small peak around December. Darling et al. (2006) reported an aberrant sinistral morphotype
264 of the dextral genotype in the North Atlantic. Although the distribution of genotypes is not known
265 for the western North Pacific, 1) the higher right-coiling ratio (42%) than at the boundary of the
266 North Atlantic (3%) and 2) a weak positive correlation ($r$ = 0.58) between coiling types (Kuroyanagi,
267 2006) suggest that most individuals were probably dextral morphologically and genetically. Seasonal
268 flux patterns for both coiling patterns of *N. pachyderma* differed from those of other major species.
269 This finding supports the hypothesis that this species inhabits a different environment or that
270 different factors control its fluxes. In particular, the lack of a prominent peak in August for *N.*

*incompta* (both coiling directions) strongly suggests that it is distinct from *N. pachyderma*, at least in the western North Pacific. This suggestion is supported by the different vertical distributions of these species around the Japanese islands (Kuroyanagi and Kawahata, 2004).

*Globolotalia scitula* had a prominent peak in the stratified summer season. Sediment trap results from Sta. B (Fig. 1) showed the maximum flux of this species in winter and early spring, with a minimum in summer (Itou et al., 2001). The seasonality difference between the two neighboring sites suggests that temperature and stratification are not major controlling factors because hydrographic conditions at intermediate depth are uniform at this scale. A common feature of the two sediment trap results is the rapid increase in *G. scitula* corresponding to a decline in particulate organic matter (POM) (Fig. 3). The sinking particles during the low POM period consist of disaggregated fine particles. Such particles have lower sinking speeds and are more likely to be preyed upon by deep dwellers (Itou et al., 2001). Longer duration in surface productivity at Sta. B probably delayed the increase in *G. scitula* until winter.

### *5.2. Estimation of vital effect on shell $\delta^{18}O$*

The $\delta^{18}O$ of planktonic foraminiferal shells is often offset from the equilibrium value, the so-called vital effect. The vital effect includes disequilibria induced by ontogeny, respiration (Spero and Lea, 1996), photosynthesis of symbionts (Spero and Lea, 1993), calcification and growth rates,

289 and carbonate chemistry (Spero et al., 1997). Because the influence of these factors on shell $\delta^{18}O$
290 largely depends on species, the magnitude of the vital effect differs among species (Niebler et al.,
291 1999). In this study, the vital effects for four species were estimated by comparing measured $\delta^{18}O$ to
292 predicted values.

293 Expansion of the depth of the mixed layer in January–March resulted in homogeneous
294 predicted $\delta^{18}O$ values for the upper 75 m (Fig. 6). If foraminiferal shells are calcified in this
295 well-mixed water, the disequilibrium can be calculated as an offset of measured $\delta^{18}O$ from the
296 predicted value. However, the calculation using $\delta^{18}O$ values from January–March was problematic.
297 The measured $\delta^{18}O$ values in February–March were comparable to those in December for all species
298 (Fig. 6). This result did not follow the predicted $\delta^{18}O$ values, which showed a continuous increase
299 until March. The discrepancy implies that shell $\delta^{18}O$ did not reflect the surface condition during this
300 period. Such discrepancies were also observed in the sediment traps moored in the subarctic North
301 Pacific (Kuroyanagi et al., 2011), the western South Pacific (King and Howard, 2005), and the
302 western subpolar North Atlantic (Jonkers et al., 2010) during small foraminiferal flux periods.
303 Therefore, we attribute these lighter $\delta^{18}O$ values to survival of the early winter population without
304 additional calcification in cold water as suggested by Jonkers et al. (2010). We decided to use $\delta^{18}O$
305 values from December and January to calculate the vital effect for the following reasons. First, the
306 predicted $\delta^{18}O$ for the upper 45 m was relatively homogeneous (Fig. 6). Second, all species analyzed

here calcify at depths < 45 m, which was deduced from the large seasonal amplitude (>1‰) in shell $\delta^{18}O$. An amplitude > 1‰ was seen only in predicted $\delta^{18}O$ values for the upper 45 m. The shallower calcification depth is supported by the concordant timing of the minimum value between measured and predicted $\delta^{18}O$ at shallower depths (Fig. 6). Third, all species showed maximum fluxes during this period, indicating that the shells trapped during this period were certainly calcified at this time. The average predicted $\delta^{18}O$ value for the upper 45 m in December and January was 1.2‰. The offsets from this predicted value were 0.0‰ for *N. pachyderma* (s) and *G. bulloides*, –0.3‰ for *N. pachyderma* (d), –0.7‰ for *N. dutertrei*, and –1.0‰ for *N. incompta* (d) (Table 1).

Previous estimates of the vital effect have not been consistent. For instance, the vital effect for the most frequently reported species, *N. pachyderma* (s), has ranged from ± 0.0 to –1.3‰. Our result is consistent with the estimation of Jonkers et al. (2010), which was obtained from a sediment trap moored in the western North Atlantic. However, other studies reported negative offsets. Ortiz et al. (1996) reported a –0.7‰ offset from California. Simstich et al. (2003) reported –0.9 and –1.0‰ offsets for encrusted and non-encrusted specimens, respectively, in the Nordic Seas. An offset of –1.0‰ was also reported from the Arctic Ocean (Bauch et al., 1997), the Okhotsk Sea (Bauch et al., 2002), the Southern Ocean (Mortyn and Charles, 2003), and the western Subarctic Gyre (Kuroyanagi et al., 2011). A much larger offset of –1.3‰ was reported from the Arctic Ocean (Volkmann and Mensch, 2001). As discussed in Kuroyanagi et al. (2011), the $\delta^{18}O$ temperature scale for calculating

the predicted $\delta^{18}O$ is an important factor. In this study, as in Jonkers et al. (2010), the $\delta^{18}O$ temperature scale of Kim and O'Neil (1997) was used because its calibrated temperature range (10, 25, and 40ºC) corresponds to the temperature of the upper layer at this site. In contrast, other high-latitude studies used the scale of O'Neil et al. (1969), which is calibrated down to 0ºC. These scales have different values, especially in the low temperature range. When calculated using the scale of O'Neil et al. (1969), the vital effect for *N. pachyderma* (s) was –0.4 ‰.

Another possibility is a difference in morphotype and/or genotype. *Neogloboquadrina incompta* has often been classified as the *N. pachyderma* dextral form. Darling et al. (2006) suggested that the left- and right-coiling forms of *N. pachyderma* should be identified as *N. pachyderma* and *N. incompta*, respectively. However, both of these species have coiling forms. For our sediment trap samples, the sinistral and dextral forms of *N. pachyderma*, *N. incompta*, and *N. dutertrei* were identified separately; the sinistral form accounted for 42%, 23%, and 23% of the species, respectively. Comparing the $\delta^{18}O$ values for two species from identical sediment trap cups, the values of *N. incompta* were ~0.7 and 0.6‰ lighter than those of *N. pachyderma* for sinistral ($n$ = 3) and dextral ($n$ = 12) forms, respectively. These results suggest that the two species have different depth habitats and/or vital effects. If one identifies *N. pachyderma* and *N. incompta* only by coiling direction, the relative abundance of the two species significantly affects mean isotope values. The genetic difference may also influence shell $\delta^{18}O$ values. Bauch et al. (2003) reported two genotypes

for *N. pachyderma* (d) in the Nordic Sea, and their $\delta^{18}O$ values had a systematic offset that may have been due to the vital effect. Although the genotype data for *N. pachyderma* in the western North Pacific have not yet been reported, the genotype of *N. pachyderma* (d) in the eastern North Pacific is distinct from that in the Atlantic (Darling et al., 2006). Therefore, differences in morphotype and/or genotype between the basins are clear candidates for geographical divergence of the vital effect.

The vital effects for the other species are also influenced by other factors, as discussed above. The values estimated in this study generally agree with those from the literature, as summarized in Niebler et al. (1999), and we provide new data on *N. incompta* (d). Significant differences in the vital effect between two morphospecies (right- and left-coiling) of *N. pachyderma*, as well as between the right-coiling forms of *N. pachyderma* and *N. incompta*, suggest that $\delta^{18}O$ measurements based on incorrect identification of these species may be a source of bias when estimating paleoceanographic conditions.

### *5.3. Estimation of calcification depths*

Calcification depths were estimated by comparing vital effect–corrected $\delta^{18}O$ values with predicted $\delta^{18}O$ values (Fig. 6). *Globigerina bulloides* $\delta^{18}O$ tracked to 45 m in June–August and to 25–35 m in October–January, with deeper values in May (Fig. 6a). Similar variation was seen in *N. pachyderma* (s) (Fig. 6d). The $\delta^{18}O$ values of *G. bulloides* and *N. pachyderma* (s) were positively

361 correlated ($r$ = 0.92). Such seasonal $\delta^{18}O$ variations suggest changes in the calcification depth in
362 response to physical or biological conditions. The large $\delta^{18}O$ changes eliminate the possibility of
363 calcification at a specific temperature because this minimizes the amplitude of seasonal $\delta^{18}O$. Rather,
364 biological conditions such as food availability probably constrained calcification depth. The
365 chlorophyll maximum at PH-1 (41º30'N, 142º00'E), which is an observational station of the Japan
366 Meteorological Agency near the study site, was ~20–30 m from May–July 2002 and 50 m from
367 April–May 2003 (Fig. 3h) (Japan Meteorological Agency, 2002, 2003). The estimated calcification
368 depths of *G. bulloides* and *N. pachyderma* (s) fell immediately below the chlorophyll maximum
369 during high-chlorophyll periods. Such vertical distributions for these species were also reported
370 around the study site using depth-discrete plankton tow experiments (Kuroyanagi and Kawahata,
371 2004) and agree with the observation that the abundance of many foraminiferal species corresponds
372 to the deep chlorophyll maximum (Fairbanks and Wiebe, 1980).

373 The vital effect–corrected $\delta^{18}O$ values for *N. incompta* (d), *N. dutertrei* (d), and *N.*
374 *pachyderma* (d) indicate calcification at 25–35-m depths throughout the year (Fig. 6b, c, e). The
375 habitat depth of *N. dutertrei* is often observed in the mixed layer to thermocline depth (e.g.,
376 Fairbanks et al., 1982; Fairbanks et al., 1980). This is also the case at the study site, where the
377 thermocline developed from 15–45 m (Fig. 2). The plankton tow experiment conducted in May–June
378 2002 showed a shallower habitat depth for *N. incompta* than for *N. pachyderma* (Kuroyanagi and

379 Kawahata, 2004). This feature was also observed in our early summer results, but is not applicable
380 for all seasons.
381
382 ***5.4. Paleoceanographic implications***
383 Our sediment trap experiment revealed significant seasonal variation in shell flux and $\delta^{18}O$ in
384 the western North Pacific. The uneven distribution of foraminiferal flux implies that
385 paleoceanographic records obtained from fossil foraminiferal $\delta^{18}O$ trend toward specific seasons.
386 Because the sedimentary $\delta^{18}O$ should reflect the weighted average of flux variation, flux-weighted
387 $\delta^{18}O$ values were calculated using equation (3) (Table 1). The flux-weighted value of 1.0‰ for *G.*
388 *bulloides* obviously reflects a large flux peak centered in December (Fig. 6a). If shells captured in
389 February and March are assumed to be survivors of early winter calcified tests, as discussed above,
390 the cumulative fluxes of the late autumn and early winter calcified shells exceeds 66% of the total
391 flux. The flux-weighted values (vital effect–corrected) for *N. dutertrei* (d) and *N. incompta* (d) were
392 1.1 and 1.2‰, respectively. These values also reflect larger fluxes centered in December, as for *G.*
393 *bulloides* (Fig. 6b, c). The cumulative fluxes from November to February reached 71% and 67‰ for
394 each species. Therefore, the sedimentary $\delta^{18}O$ values for three species, *G. bulloides*, *N. dutertrei* (d),
395 and *N. incompta* (d), record surface temperatures mainly in early winter with species-specific vital
396 effect offsets.

397 The case of *N. pachyderma* is more complicated owing to broad flux peaks. The
398 flux-weighted value for *N. pachyderma* (s) was 1.4‰. Measured $\delta^{18}O$ values for June–August and
399 December–March were around 1.4‰ (Fig. 6d). The cumulative fluxes of the former and latter
400 periods account for 58% and 28% of the total flux, respectively, indicating that the sedimentary $\delta^{18}O$
401 value of this species reflects surface temperature primarily in summer and secondarily in early winter.
402 The flux-weighted value for *N. pachyderma* (d) was 0.8‰. The prominent peak in August accounts
403 for 18.4% and the broad peak in October–January accounts for 63% of the total flux. The broad
404 distribution of shell flux suggests that the sedimentary $\delta^{18}O$ value indicates mean annual temperature
405 at 25–45 m.

406 The sedimentary $\Delta\delta^{18}O$ of foraminiferal species, according to differences in habitat depth or
407 season, is often used to deduce past ocean stratification conditions or seasonality. The estimated
408 calcification depths for the four species examined in this study ranged from 25 to 45 m (Table 1).
409 Small divergences in calcification depths suggest that the sedimentary $\Delta\delta^{18}O$ does not provide a
410 proxy for past stratification in this region, unlike other areas (e.g., Southern Ocean) where depth
411 habitat differences are large enough between species that stratification changes can be deduced
412 (Mortyn and Charles, 2003; Mortyn et al., 2002). The only candidate for a temperature recorder at
413 intermediate depth is *G. scitula*. Although the $\delta^{18}O$ for this species was not provided in this study
414 because of discontinuous occurrence during the sampling period, the examination of depth habitat

and shell chemistry by Itou et al. (2001) suggested *G. scitula* as an intermediate depth indicator. If one combines the $\delta^{18}O$ values of *G. scitula* and *N. pachyderma* (s), which primarily reflect summer subsurface and surface temperature, respectively, $\Delta\delta^{18}O$ may provide a proxy for summer stratification. In contrast to the calcification depth, the seasonal flux differences among species are observed. The difference in seasonal preference of *N. pachyderma* (s) from other species may provide a seasonal contrast for surface to subsurface water in the western North Pacific. Namely, the $\Delta\delta^{18}O$ between *N. pachyderma* (s) and other winter species [*G. bulloides*, *N. dutertrei* (d), and *N. incompta* (d)] possibly records a contrast between summer and early winter. This study revealed that the seasonal variation of foraminiferal flux was strongly affected by the regional oceanographic variations. Therefore, added modern perspectives on a regional basis will help in more precise paleoceanographic reconstructions.

## 6. Summary

In this study, we investigated the seasonal variation in foraminiferal flux and $\delta^{18}O$ using a 1-year data set from a moored sediment trap in the northwestern North Pacific. The TFF had three distinct peaks centered in June, August, and December. Six major species (*N. incompta*, *N. dutertrei*, *N. pachyderma*, *G. quinqueloba*, *G. bulloides*, and *G. scitula*) constituted 97% of the TFF. All species except *G. scitula*, which had only one prominent peak in August, showed higher fluxes in June and

December. Additional peaks in August were observed for *N. dutertrei* and *N. pachyderma*. The seasonal successions of foraminiferal fluxes correspond to surface ocean stratification and food availability, which are closely related to local current circulation. Comparison of seasonal $\delta^{18}O$ variations in foraminiferal shells with predicted values, calculated using temperature and $\delta^{18}O$ of seawater, revealed species-specific vital effects and calcification depths. The vital effect estimations suggest that shells calcified in equilibrium for *G. bulloides* and *N. pachyderma* (s) and with a –0.7‰ offset for *N. dutertrei* (d), a –1.0‰ offset for *N. incompta* (d), and a –0.3‰ offset for *N. pachyderma* (d). Differences in seasonal flux pattern and the vital effect between *N. pachyderma* (d) and *N. incompta* (d) suggest that separation of these species only by coiling direction is a source of bias in the estimation of paleoceanographic conditions in this region. The flux-weighted $\delta^{18}O$ values suggest that sedimentary $\delta^{18}O$ in three species [*G. bulloides*, *N. dutertrei* (d), and *N. incompta* (d)] mainly record temperatures in the surface layer in early winter, with species-specific vital effect offsets. The sedimentary $\delta^{18}O$ values of *N. pachyderma* (s) and (d) record summer subsurface and mean annual subsurface temperatures, respectively. The surface calcification of the four species implies the potential to reconstruct past seasonality, in particular via $\Delta\delta^{18}O$ between *N. pachyderma* (s) and *G. bulloides*, *N. dutertrei* (d) or *N. incompta* (d). The prominent peak in summer for *G. scitula* implies that the $\delta^{18}O$ difference compared to the subsurface species *N. pachyderma* (s) may provide a proxy for summer surface stratification.

## Acknowledgments

We thank the onboard scientists, officers, and crew of the R/V *Kairei* for help with sampling. We also thank N. Hokanishi for her assistance in the laboratory. We are grateful to the Editor Richard Jordan and reviewers Graham Mortyn and Dorothea Bauch for their insightful comments. This study is partly supported by Special Coordination Funds for Promoting Science and Technology to M.K. funded by the Ministry of Education, Culture, Sports, Science, and Technology and by the Grant-in-Aid for Scientific Research (S) of 22224009 to H.K. funded by the Japan Society for the promotion of science.

## References

Bauch, D., Carstens, J., Wefer, G., 1997. Oxygen isotope composition of living *Neogloboquadrina pachyderma* (sin.) in the Arctic Ocean. Earth and Planetary Science Letters 146, 47-58.

Bauch, D., Darling, K., Simstich, J., Bauch, H.A., Erlenkeuser, H., Kroon, D., 2003. Palaeoceanographic implications of genetic variation in living North Atlantic *Neogloboquadrina pachyderma*. Nature 424, 299-302.

Bauch, D., Erlenkeuser, H., Winckler, G., Pavlova, G., Thiede, J., 2002. Carbon isotopes and habitat of polar planktic foraminifera in the Okhotsk Sea: the 'carbonate ion effect' under natural conditions. Marine Micropaleontology 45, 83-99.

Behringer, D., Xue, Y., 2004. Evaluation of the global ocean data assimilation system at NCEP: the

Pacific Ocean, Eighth Symposium on Integrated Observing and Assimilation Systems for Atmosphere, Oceans, and Land Surface, AMS 84th Annual Meeting, Washington State Convention and Trade Center, Seattle, Washington, pp. 1-6.

Bemis, B.E., Spero, H.J., Bijma, J., Lea, D.W., 1998. Reevaluation of the oxygen isotopic composition of planktonic foraminifera: Experimental results and revised paleotemperature equations. Paleoceanography 13, 150-160.

Darling, K.F., Kucera, M., Kroon, D., Wade, C.M., 2006. A resolution for the coiling direction paradox in *Neogloboquadrina pachyderma*. Paleoceanography 21, PA2011, doi:10.1029/2005PA001189.

Darling, K.F., Wade, C.M., Stewart, I.A., Kroon, D., Dingle, R., Leigh Brown, A.J., 2000. Molecular evidence for genetic mixing of Arctic and Antarctic subpolar populations of planktonic foraminifers. Nature 405, 43-47.

Epstein, S., Buchsbaum, R., Lowenstam, H.A., Urey, H.C., 1953. Revised carbonate-water isotopic temperature scale. Bulletin of the Geological Society of America 64, 1315-1326.

Fairbanks, R.G., Sverdlove, M., Free, R., Wiebe, P.H., Be, A.W.H., 1982. Vertical distribution and isotopic fractionation of living planktonic foraminifera from the Panama Basin. Nature 298, 841-844.

Fairbanks, R.G., Wiebe, P.H., 1980. Foraminifera and Chlorophyll Maximum: Vertical Distribution, Seasonal Succession, and Paleoceanographic Significance. Science 209, 1524-1526.

Fairbanks, R.G., Wiebe, P.H., Be, A.W.H., 1980. Vertical distribution and isotopic composition of living planktonic foraminifera in the western north Atlantic. Science 207, 61-63.

Hanawa, K., Mitsudera, H., 1986. Variation of water system distribution in the Sanriku Coastal Area. Journal of the Oceanographical Society of Japan 42, 435-446.

Hemleben, C., Spindler, M., Anderson, O.R., 1989. Modern planktonic foraminifera. Springer-Verlag, New York, p. 363.

Hilbrecht, H., 1997. Morphologic gradation and ecology in *Neogloboquadrina pachyderma* and *N.*

*dutertrei* (planktic foraminifera) from core top sediments. Marine Micropaleontology 31, 31-43.

Hut, G., 1987. Consultants' group meeting on stable isotope reference samples for geochemical and hydrological investigations, Report to the Director General. International Atomic Energy Agency, Vienna, p. 42.

Itaki, T., Minoshima, K., Kawahata, H., 2008. Radiolarian flux at an IMAGES site at the western margin of the subarctic Pacific and its seasonal relationship to the Oyashio Cold and Tsugaru Warm currents. Marine Geology 255, 131-148.

Itou, M., Noriki, S., 2002. Shell fluxes of solution-resistant planktonic foraminifers as a proxy for mixed-layer depth. Geophysical Research Letters 29, 19-11.

Itou, M., Ono, T., Oba, T., Noriki, S., 2001. Isotopic composition and morphology of living *Globorotalia scitula*: A new proxy of sub-intermediate ocean carbonate chemistry? Marine Micropaleontology 42, 189-210.

Jonkers, L., Brummer, G.-J.A., Peeters, F.J.C., van Aken, H.M., De Jong, M.F., 2010. Seasonal stratification, shell flux, and oxygen isotope dynamics of left-coiling *N. pachyderma* and *T. quinqueloba* in the western subpolar North Atlantic. Paleoceanography 25, PA2204, doi:10.1029/2009PA001849.

Kawahata, H., Minoshima, K., Ishizaki, Y., Yamaoka, K., Gupta, L.P., Nagao, M., Kuroyanagi, A., 2009. Comparison of settling particles and sediments at IMAGES coring site in the northwestern North Pacific — Effect of resuspended particles on paleorecords. Sedimentary Geology 222, 254-262.

Kawahata, H., Yamamuro, M., Ohta, H., 1998. Seasonal and vertical variations of sinking particle fluxes in the West Caroline Basin. Oceanologica Acta 21, 521-532.

Kim, S.-T., O'Neil, J.R., 1997. Equilibrium and nonequilibrium oxygen isotope effects in synthetic carbonates. Geochimica et Cosmochimica Acta 61, 3461-3475.

King, A.L., Howard, W.R., 2005. $\delta^{18}O$ seasonality of planktonic foraminifera from Southern Ocean sediment traps: Latitudinal gradients and implications for paleoclimate reconstructions. Marine

519 Micropaleontology 56, 1-24.
520 Kono, T., Foreman, M., Chandler, P., Kashiwai, M., 2004. Coastal Oyashio South of Hokkaido, Japan.
521 Journal of Physical Oceanography 34, 1477-1494.
522 Kuroyanagi, A., 2006. Spatial and seasonal distribution of planktonic foraminifera *Neogloboquadrina*
523 *pachyderma* in the northwestern Pacific and reconstruction of paleoceanography off Shimokita. Fossils,
524 21-32, (in Japanese with English abstract).
525 Kuroyanagi, A., Kawahata, H., 2004. Vertical distribution of living planktonic foraminifera in the seas
526 around Japan. Marine Micropaleontology 53, 173-196.
527 Kuroyanagi, A., Kawahata, H., Narita, H., Ohkushi, K., Aramaki, T., 2006. Reconstruction of
528 paleoenvironmental changes based on the planktonic foraminiferal assemblages off Shimokita (Japan) in
529 the northwestern North Pacific. Global and Planetary Change 53, 92-107.
530 Kuroyanagi, A., Kawahata, H., Nishi, H., 2011. Seasonal variation in the oxygen isotopic composition of
531 different-sized planktonic foraminifer *Neogloboquadrina pachyderma* (sinistral) in the northwestern
532 North Pacific and implications for reconstruction of the paleoenvironment. Paleoceanography 26, PA4215,
533 doi:10.1029/2011PA002153.
534 Kuroyanagi, A., Kawahata, H., Nishi, H., Honda, M.C., 2002. Seasonal changes in planktonic
535 foraminifera in the northwestern North Pacific Ocean: Sediment trap experiments from subarctic and
536 subtropical gyres. Deep-Sea Research Part II: Topical Studies in Oceanography 49, 5627-5645.
537 Kuroyanagi, A., Kawahata, H., Nishi, H., Honda, M.C., 2008. Seasonal to interannual changes in
538 planktonic foraminiferal assemblages in the northwestern North Pacific: Sediment trap results
539 encompassing a warm period related to El Niño. Palaeogeography, Palaeoclimatology, Palaeoecology 262,
540 107-127.
541 McCrea, J.M., 1950. On the Isotopic Chemistry of Carbonates and a Paleotemperature Scale. The Journal
542 of Chemical Physics 18, 849-857.

543 Mortyn, P.G., Charles, C.D., 2003. Planktonic foraminiferal depth habitat and $\delta^{18}O$ calibrations: Plankton
544 tow results from the Atlantic sector of the Southern Ocean. Paleoceanography 18, 1037,
545 doi:10.1029/2001PA000637.
546 Mortyn, P.G., Charles, C.D., Hodell, D.A., 2002. Southern Ocean upper water column structure over the
547 last 140 kyr with emphasis on the glacial terminations. Global and Planetary Change 34, 241-252.
548 Mulitza, S., Dürkoop, A., Hale, W., Wefer, G., Niebler, H.S., 1997. Planktonic foraminifera as recorders of
549 past surface-water stratification. Geology 25, 335-338.
550 Niebler, H.-S., Hubberten, H.-W., Gersonde, R., 1999. Oxygen isotope valuse of planktic foraminifera: A
551 tool for the reconstruction of surface water stratification, In: Fischer, G., Wefer, G. (Eds.), Use of Proxies
552 in Paleoceanography: Examples from the South Atlantic. Springer, New York, pp. 165-189.
553 O'Neil, J.R., Clayton, R.N., Mayeda, T.K., 1969. Oxygen Isotope Fractionation in Divalent Metal
554 Carbonates. The Journal of Chemical Physics 51, 5547-5558.
555 Oba, T., Murayama, M., 2004. Sea-surface temperature and salinity changes in the northwest Pacific since
556 the last glacial maximum. Journal of Quaternary Science 19, 335-346.
557 Oda, M., Domitsu, H., 2009. Paleoceanographic significance of *Neogloboquaderina pachyderma* and
558 *Neogloboquaderina incompta*. Fossils 86, 6-11, (in Japanese with English abstract).
559 Ortiz, J.D., Mix, A.C., Rugh, W., Watkins, J.M., Collier, R.W., 1996. Deep-dwelling planktonic
560 foraminifera of the northeastern Pacific Ocean reveal environmental control of oxygen and carbon
561 isotopic disequilibria. Geochimica et Cosmochimica Acta 60, 4509-4523.
562 Park, B.-K., Shin, I.C., 1998. Seasonal distribution of planktic foraminifers in the East Sea (Sea of Japan),
563 a large marginal sea of the northwest Pacific. Journal of Foraminiferal Research 28, 321-326.
564 Parker, F.L., 1962. Planktonic foraminiferal species in Pacific sediments. Micropaleontology 8, 219-254.
565 Rashid, H., Boyle, E.A., 2007. Mixed-Layer Deepening During Heinrich Events: A Multi-Planktonic
566 Foraminiferal $\delta^{18}O$ Approach. Science 318, 439-441.

567 Sagawa, T., Yokoyama, Y., Ikehara, M., Kuwae, M., 2011. Vertical thermal structure history in the
568 western subtropical North Pacific since the Last Glacial Maximum. Geophys. Res. Lett. 38, L00F02,
569 doi:10.1029/2010GL045827.
570 Saito, T., Thompson, P.R., Breger, D., 1981. Systematic index of recent and Pleistocene planktonic
571 foraminifera. University of Tokyo Press, Tokyo, p. 175.
572 Sautter, L.R., Thunell, R.C., 1991. Seasonal variability in the δ18O and δ13C of planktonic foraminifera
573 from an upwelling environment: sediment trap results from the San Pedro Basin, southern California
574 Bight. Paleoceanography 6, 307-334.
575 Simstich, J., Sarnthein, M., Erlenkeuser, H., 2003. Paired $\delta^{18}O$ signals of *Neogloboquadrina pachyderma*
576 (s) and *Turborotalita quinqueloba* show thermal stratification structure in Nordic Seas. Marine
577 Micropaleontology 48, 107-125.
578 Spero, H.J., Bijma, J., Lea, D.W., Bernis, B.E., 1997. Effect of seawater carbonate concentration on
579 foraminiferal carbon and oxygen isotopes. Nature 390, 497-500.
580 Spero, H.J., Lea, D.W., 1993. Intraspecific stable isotope variability in the planktic foraminifera
581 *Globigerinoides sacculifer*: results from laboratory experiments. Marine Micropaleontology 22, 221-234.
582 Spero, H.J., Lea, D.W., 1996. Experimental determination of stable isotope variability in *Globigerina*
583 *bulloides*: Implications for paleoceanographic reconstructions. Marine Micropaleontology 28, 231-246.
584 Spero, H.J., Mielke, K.M., Kalve, E.M., Lea, D.W., Pak, D.K., 2003. Multispecies approach to
585 reconstructing eastern equatorial Pacific thermocline hydrography during the past 360 kyr.
586 Paleoceanography 18, 1022, doi:10.1029/2002PA000814.
587 Thompson, P.R., Shackleton, N.J., 1980. North Pacific palaeoceanography: late Quaternary coiling
588 variations of planktonic foraminifer *Neogloboquadrina pachyderma*. Nature 287, 829-833.
589 Volkmann, R., Mensch, M., 2001. Stable isotope composition ($\delta^{18}O$, $\delta^{13}C$) of living planktic foraminifers
590 in the outer Laptev Sea and the Fram Strait. Marine Micropaleontology 42, 163-188.

591 von Langen, P., Lea, D.W., Spero, H.J., 2000. Effects of temperature on oxygen isotope and Mg/Ca values
592 in *Neogloboquadrina pachyderma* shells determined by live culturing, AGU Fall Meeting, San Francisco,
593 pp. OS11C-20.
594 Yasuda, I., 2003. Hydrographic structure and variability in the Kuroshio-Oyashio Transition Area. Journal
595 of Oceanography 59, 389-402.
596
597 Figure captions
598 Figure 1. Maps showing the study site and surface current systems in the western North Pacific. (a)
599 Major surface currents in the study region. The rectangle with broken line indicates the
600 area shown in the inset. (b) The locations of the sediment trap used in this study and
601 reference site Sta. B. Three rectangles are 1°×1°grids of NCEP GODAS used for the
602 predicted $\delta^{18}O$ calculation in Fig. 2 and Fig. 6. TWC: Tsushima Warm Current, TGC:
603 Tsugaru Warm Current.
604 Figure 2. Seasonal variation in temperature (a), salinity (b), potential density (c), and predicted
605 oxygen isotopic composition ($\delta^{18}O$) of equilibrium calcite (d) for the upper 200 m. The
606 temperature and salinity data are averages of three grids in Fig. 1 obtained from the
607 National Centers for Environmental Prediction Global Ocean Data Assimilation System
608 (Behringer and Xue, 2004). The predicted $\delta^{18}O$ values were calculated using the equation
609 of Kim and O'Neil (1997) (see text for details).
610 Figure 3. Flux variation in major components of sediment trap samples. Fluxes in (a) total mass, (b)
611 lithogenics, (c) biogenic opal, (d) organic matter, (e) carbonate, and (f) total foraminifera.

(g) Temperature variation to 200 m water depth during the mooring period (data from the Global Ocean Data Assimilation System). (h) Variation in chlorophyll-*a* concentration for the upper 100 m measured at station PH-1 (41°30'N, 142°00'E) on 27 April 2002, 19 July 2002, 5 October 2002, 2 December 2002, 8 February 2003, 2 May 2003, and 4 August 2003 by the Japan Meteorological Agency. Vertical white lines indicate observational dates during the mooring period. The data are temporally interpolated to intervals of one week with the surface tool in the Generic Mapping Tools. Data for (a)–(e) are from (Kawahata et al., 2009). Sample cup numbers are shown in (a).

Figure 4. Flux variation in total foraminifera and the six major species. The two morphospecies of *Neogloboquadrina pachyderma*, *N. incompta*, and *N. dutertrei* are shown in separate panels. Dark and light colors represent shell sizes > 250 μm and 125–250 μm, respectively.

Figure 5. The results of $\delta^{18}O$ replicate analyses. Each data point consists of 4-13 specimens with mostly less than 10 specimens. The $\delta^{18}O$ are normalized by subtracting average values for the purpose of comparison. The standard deviations (1σ) are shown on the right side of each data.

Figure 6. Seasonal variation in oxygen isotopes (dots) and shell flux (bars) for (a) *Globigerina bulloides*, (b) *Neogloboquadrina incompta* (dextral), (c) *N. dutertrei* (dextral), (d) *N. pachyderma* (sinistral), and (e) *N. pachyderma* (dextral) of small shell size (125–250 μm).

The vital effect–corrected oxygen isotopic composition ($\delta^{18}O$) values are also shown in (b), (c), and (e). Lines show seasonal variation of the predicted $\delta^{18}O$ values for the upper ~300 m. Error bars in (d) and (e) show the standard deviation (1σ) of replicate analyses.

635

636 Table 1. The estimations of vital effect, depth habitat, and flux–weighted $\delta^{18}O$ value.

| Species | Vital effect (‰) | Estimated depth habitat (m) | Flux–weighted $\delta^{18}O$ value (‰) |
|---|---|---|---|
| *G. bulloides* | 0.0 | ~45 (Jun-Aug)<br>25-35 (Oct-Jan) | 1.0 |
| *N. dutertrei* (d) | -0.7 | 25-35 | 1.1* |
| *N. incompta* (d) | -1.0 | 25-35 | 1.2* |
| *N. pachyderma* (d) | -0.3 | 25-35 | 0.8* |
| *N. pachyderma* (s) | 0.0 | 35-45 (Jun-Aug)<br>~35 (Oct-Jan) | 1.4 |

637 * vital effect corrected (see section 5.4)

638

639

Figure 1 Sagawa et al.

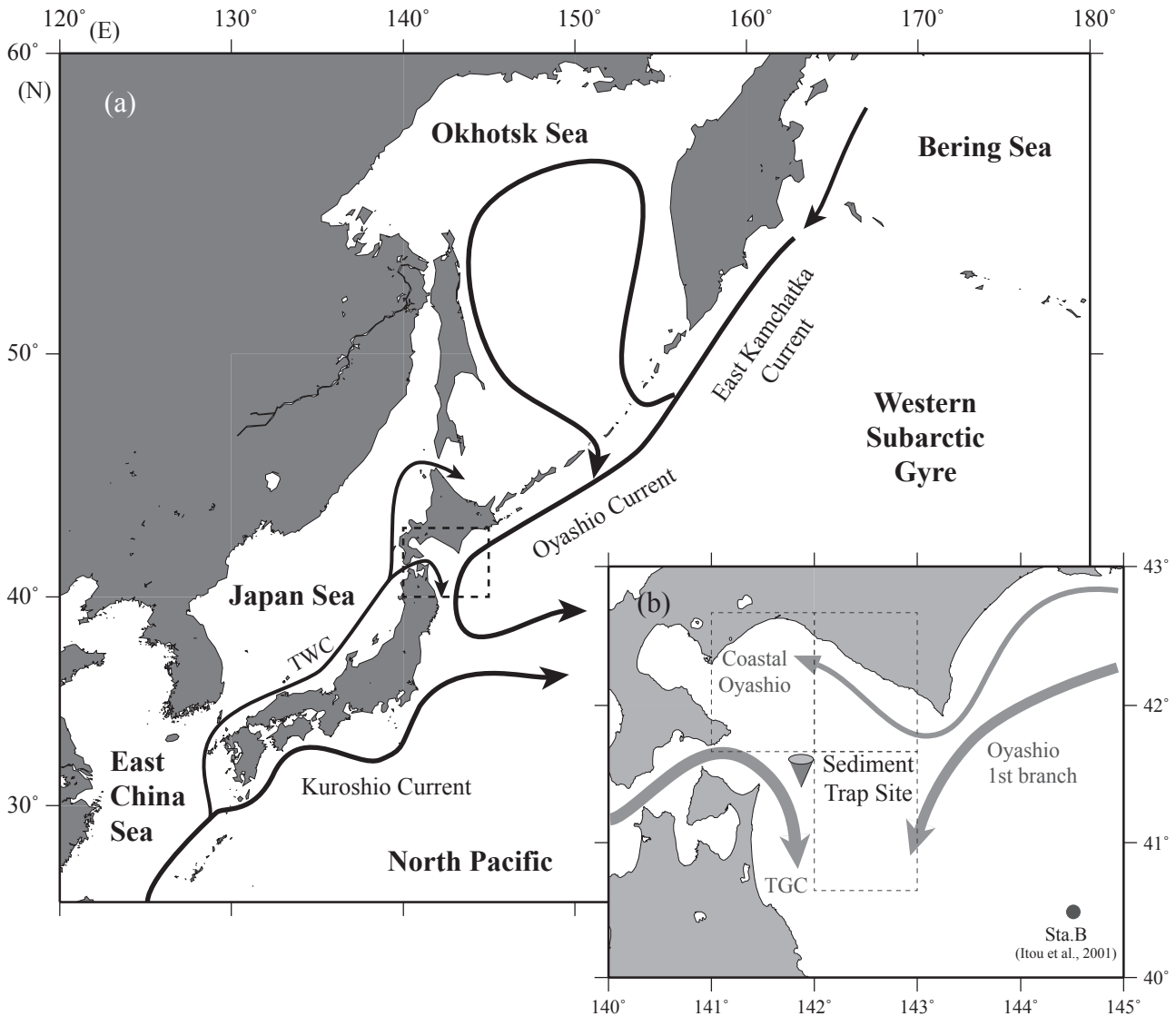

Figure 2 Sagawa et al.

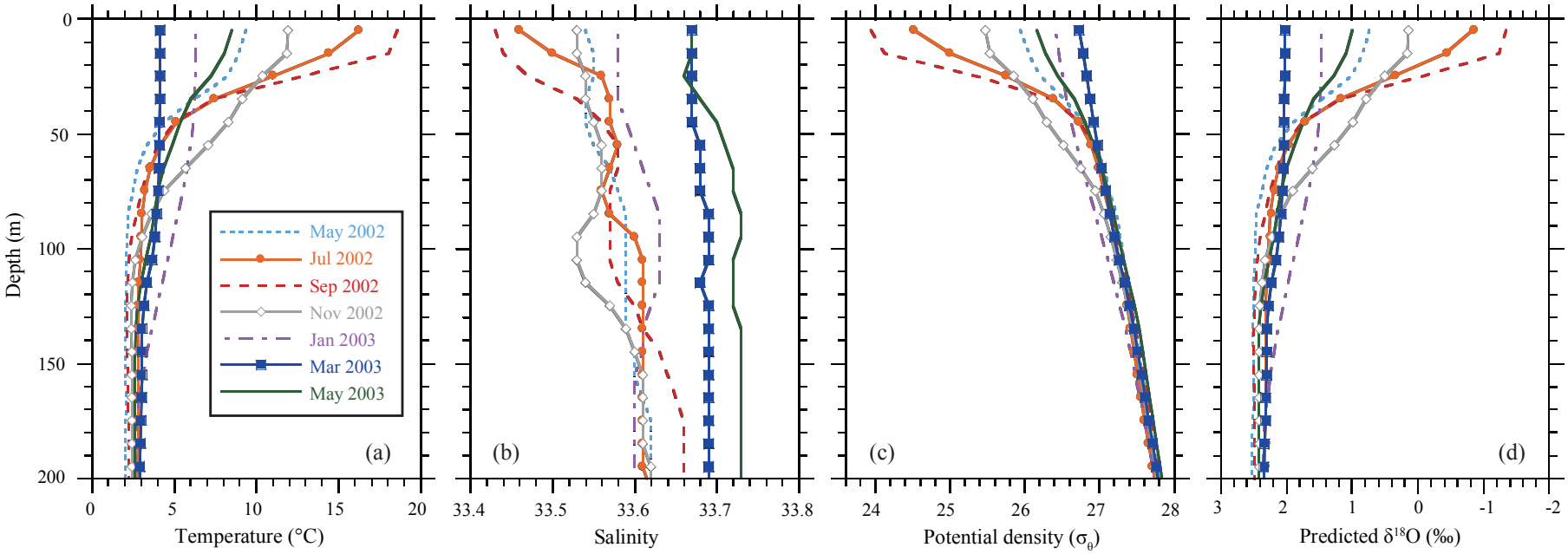

Figure 3 Sagawa et al.

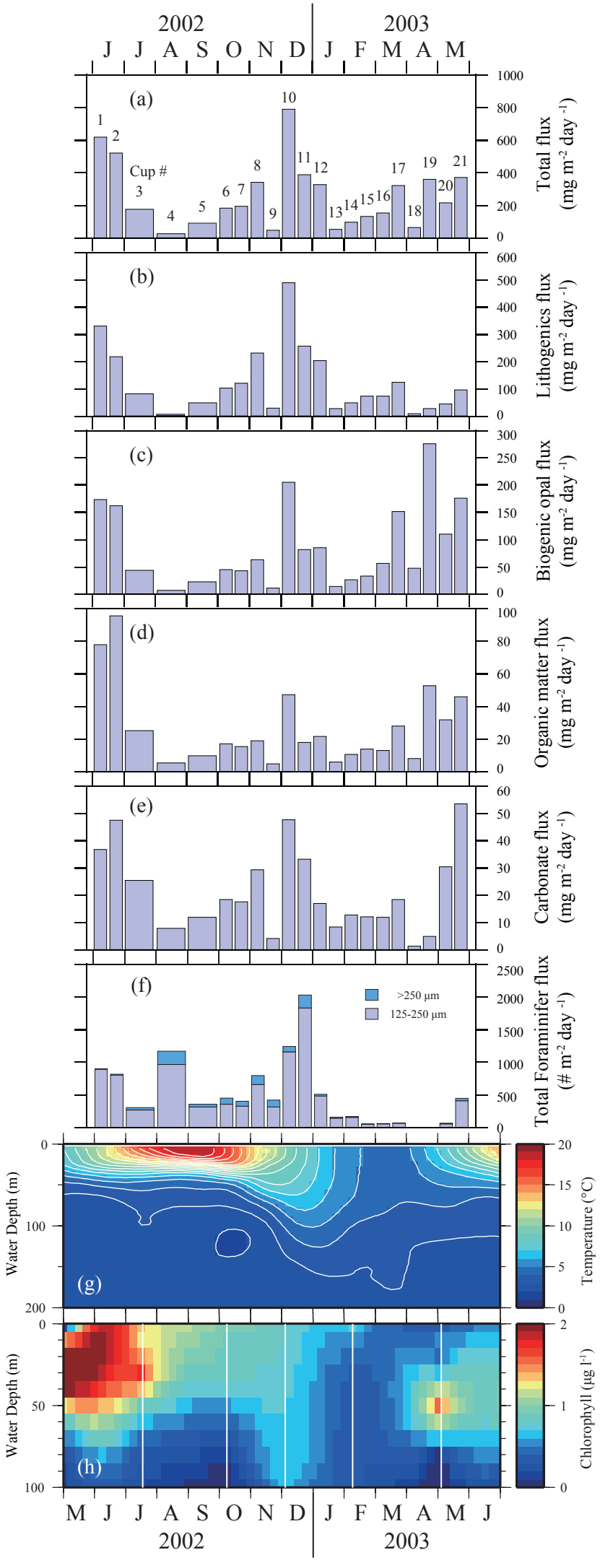

Figure 4 Sagawa et al.

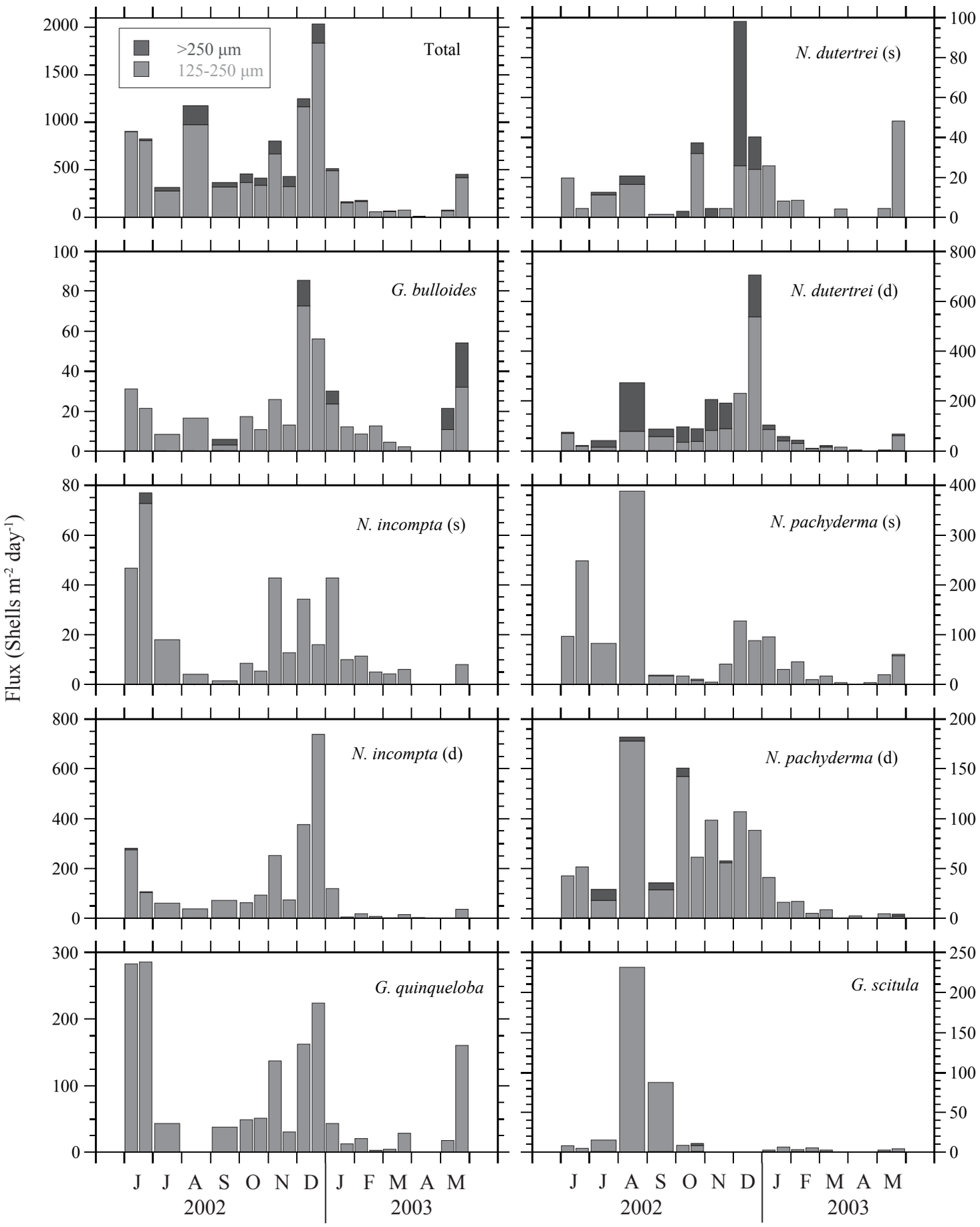

Figure 5 Sagawa et al.

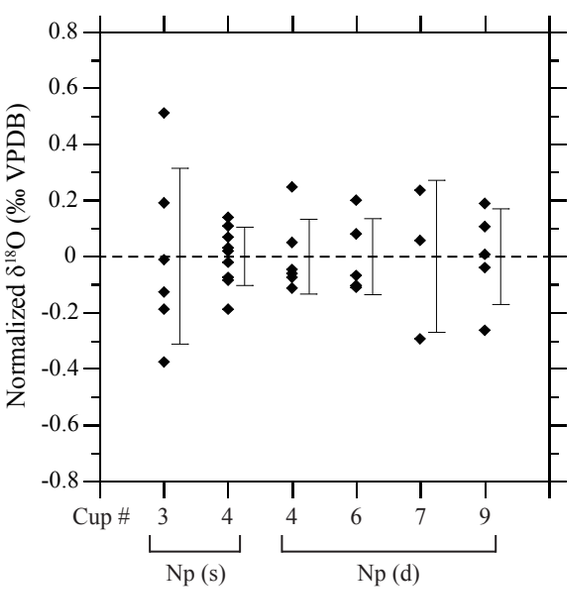

Figure 6 Sagawa et al.